Large Scale Prototyping in the Oil & Gas Industry: The Use of FEA in the Structural Capacity Rating of a Deep Sea Pipeline Clamping System

Dr. David Winfield[1], Laurence Marks[2], John Stobbart[1] and Nick Long[1]

[1]Freudenberg Oil & Gas Technologies Ltd, Unit 18, Baglan Industrial Estate, Baglan, Port Talbot, SA12 7BY, United Kingdom

[2]Strategic Simulation and Analysis Ltd, Southill Barn, Southill Business Park, Cornbury Park, Charlbury, Oxfordshire, OX7 3EW, United Kingdom

***Abstract**: Freudenberg Oil & Gas Technologies (FO&GT) in Port Talbot, UK, provides complex metal to metal sealing solutions for the oil & gas and energy industries. FO&GT is supplying two of its largest Optima® subsea connectors for use just inside the Arctic Circle. These will be the deepest of their kind anywhere in the world.*

Weighing some 10 tons, the Optima® is a high precision, multi-piece clamping system using a FO&GT Duoseal® metallic seal, tensioned by multiple leadscrew(s), activated via integral drive buckets. The resulting leadscrew tension positions the clamp segments on the hubs; as the tension increases, the opposing hubs are pulled together overcoming external forces and moments. Pressure energisation and plastic deformation ensure a high integrity double seal between the inner pipeline and the deep water environment.

Multi-body elasto-plastic finite element analysis (FEA) is used to simulate the interaction and contact between all parts of the Optima®, with focus on the stress and plastic strain of individual components during make-up and operation.

Fluctuating in-service loadings such as temperature, pressure and bending moment are also analyzed to qualify the clamp segments, together with capacity analysis for the clamps and Duoseal®, where contact analysis is used to verify Duoseal® compliance. The Optima® is also required to overcome a range of hub misalignments, resulting from installation tolerances, friction and pipeline flexibility.

The FEA simulation results of the Optima® will be used to support experimental test data obtained during factory trials, prequalifying these components to the most extreme subsea loading conditions.

***Keywords**: Subsea, Clamping, Plasticity, Dynamic Implicit, Multi-Body Dynamics, Connectors, Coupled Analysis, Design Optimization, Interface Friction, Oil & Gas, Pipeline, Sealing, Metallic Seals, Abaqus/CAE.*

1. Introduction

Freudenberg Oil & Gas Technologies Ltd (FO&GT) specializes in a range of high precision metal to metal sealing solutions, including seal rings, pipe connectors and flanges, as well as full assemblies of a range of high capacity Optima subsea connectors. Oil and gas pipeline operation requires high integrity sealing solutions to cope with the fluctuating demands of transport media, pressure and temperature to match the campaign life required by the customer. With oil and gas resources becoming increasingly more difficult to find and extract, pipeline components must be designed to cope with the increased demands of deeper and rougher waters.

As well as the analysis of specialist subsea equipment, FO&GT have used Abaqus/CAE to undertake coupled thermal-structural FEA simulations for ultra-high temperature applications (1600 F) utilizing custom flange and connector designs, together with bespoke kammprofile gaskets, producing highly reliable sealing solutions whilst subjected to severe in-service loadings. FO&GT has also analyzed, bespoke sealing solutions for harsh environment chemical mixing and reaction vessels up to 65,000 Psi.

FO&GT has been approached to design and specify a pair of No.36 Optima subsea connectors for an application in the Norwegian Sea, just inside the Arctic Circle. The No.36 Optima that FO&GT are analyzing and supplying, will be both the largest and deepest of its kind installed anywhere in the world; it is expected that the Optima will be subjected to operating depths of nearly 4,000 feet, in some of the harshest deep sea conditions. Due to the simple design of the Optima and the use of a FO&GT DuoSeal®, complex multi-body finite element analysis (FEA) is required to be undertaken with Abaqus/CAE to qualify the components of interest.

The design of the No.36 Optima is based on a similar qualified clamp size for a previous customer request. The design challenges look to incorporate a new clamping and leadscrew arrangement, being subjected to a pressure depth FO&GT have never supplied to before. Previous FEA work undertaken on the earlier customer design was done externally, but with FO&GT now undertaking FEA simulation work completely in-house, the modeling methodology has been extensively fine-tuned, and the results generated through the FEA can be checked periodically with theory, ensuring the accuracy of the settings used to predict the resultant solution.

FEA simulation has been undertaken on a range of similar individual components and principles, such as lip seals (Chun-Ying Lee, 2006), (Chung Kyun Kim, 1997), clamping pressure distribution (Alex Bates, 2013), together with general analysis of pressure vessels (Sanal, 2000).

This paper addresses the problem of analyzing an optimized FO&GT design which has been tailored to provide a high capacity sealing solution to the customer, whilst remaining light-weight and easy to manufacture. FEA simulation provides a robust, cost effective and non-invasive method of structural interrogation, especially when components and systems must be taken to the point of failure and structural collapse. The paper also documents how the Optima's are assessed from an FEA perspective, presenting results on the optimized No.36 Optima, designed to meet customer specification. Rated capacity procedures for the No.36 Optima are detailed, together with how the FEA results and proposed factory testing validate one another. A summary of the

function and location within the pipeline system of the No.36 Optima is followed by an overview of the problems encountered during the modeling process causing inconsistent, or, very little convergence is discussed. Contact stabilization, mass effects and time step lengths, together with the processes and settings required to overcome some of the more complex convergence problems are reviewed, that finally generate a repeatable and reliable solution.

2. Deep Sea Pipeline/Clamping System Layout and No.36 Optima

The pipeline/clamping system is illustrated in Figure 1;

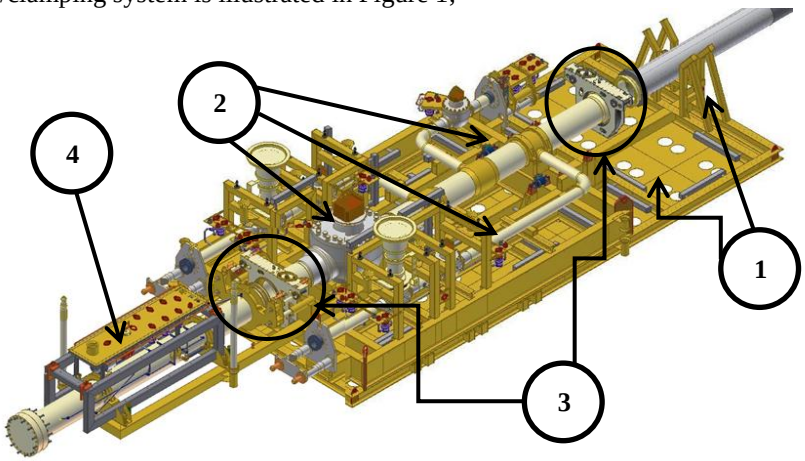

Figure 1: Illustration of the deep sea pipeline/clamping system with the four major structures identified.

The system constitutes four major elements; the frame support platform (FSP) complete with 'cow horns' to support the main gas pipeline (**1**), the pipeline module (PLEM), which is pre-constructed and lowered onto a set of friction pads incorporated into the FSP (**2**), a pair of No.36 FO&GT Optima's (**3**), and the pig launcher which is connected to the rear end of the PLEM (**4**).

2.1 No.36 Optima; Principles of Operation

The No.36 Optima (*see Figure 2*) is a high precision, multi-piece clamping system using a FO&GT DuoSeal metallic seal between opposing male and female hubs. The clamping segments are locked around the hubs using the tension generated by threaded leadscrew(s) and trunnion(s), actuated via a suitable subsea tooling interface. Resulting leadscrew tension aligns and positions the clamp segments over the hubs. As leadscrew tension increases, opposing hubs are displaced towards each other, overcoming large external forces and moments.

Inward displacement of opposing hubs generates elasto-plastic deformation in the DuoSeal, creating the initial seal on the inner/outer heel regions. When subjected to internal pressure, pressure energisation together with plastic deformation ensures a high integrity double seal between the inner pipeline and external deep water environment. Movement of the trunnion(s) and

link-pin is directed via guide slots cut into the supporting enclosure. Once assembled the Optima is freely supported by the enclosure alone.

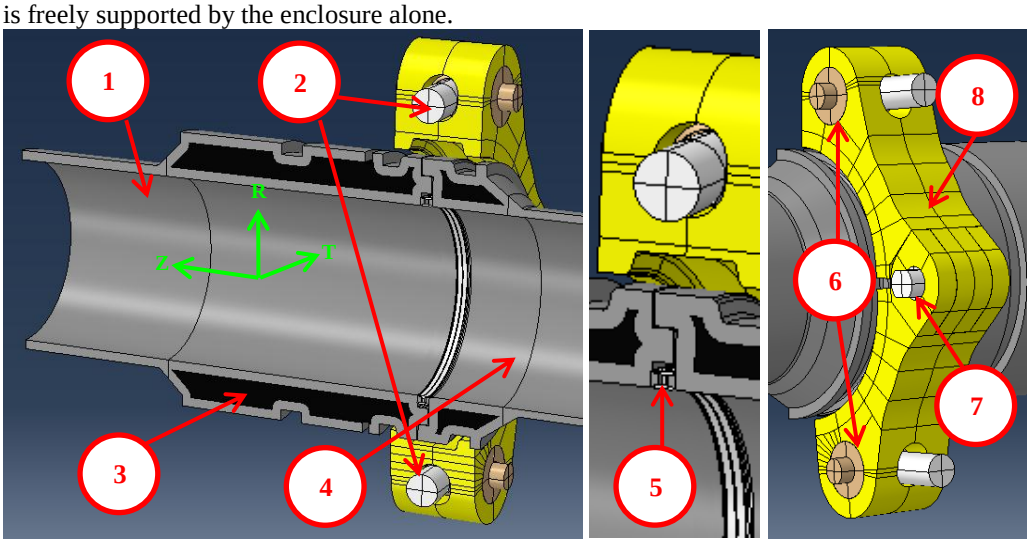

Figure 2: Left to right: schematic symmetry plan view of the No.36 Optima and cylindrical co-ordinate system, close-up of hub, seal and clamp geometry detail, external view of clamp segments.

The Optima enclosure is nominally 96 inches square, by 25 inches deep. The No.36 Optima has an internal bore of 34 inches and an external hub diameter of 50 inches. The whole assembly weighs approximately $22x10^3$ Lbs (10 tons). Component materials are identified in Table 1;

Table 1: No.36 Optima components and materials.

Region	Optima Component	Material Specification	Young's Modulus (Psi)	Yield Stress (Psi)
1	Male Hub and Pipe	ASTM A694 F65	$30.5x10^6$	$71.4x10^3$
2	Leadscrew(s)	Inconel 725 (UNS N07725)	$30.3x10^6$	$116.0x10^3$
3	Inner forging (black regions)	ASTM A694 F65	$30.5x10^6$	$65.7x10^3$
4	Female Hub and Pipe	ASTM A694 F65	$30.5x10^6$	$71.4x10^3$
5	DuoSeal	Inconel 725 (UNS N07725)	$30.3x10^6$	$116.0x10^3$
6	Trunnion(s)	Hiduron 130	$20.2x10^6$	$100.8x10^3$
7	Link-pin	Inconel 725 (UNS N07725)	$30.3x10^6$	$116.0x10^3$
8	Clamp Segments	AISI 4140	$30.5x10^6$	$75.0x10^3$

The geometry model utilizes inner forging regions (*see Figure 2*) specified by FO&GT. These inner regions have a slightly lower yield point than the outer portion of the hub(s) due to the manufacturing process associated with the forging (heat treatment, water quench and tempered).

3. Outline of the FEA Model

3.1 FEA Sub-Modeling

The FEA modeling methodology began life with a series of less complex sub models of different interacting parts of the Optima. This included hub-on-DuoSeal contact, clamp-on-hub contact, clamp-on-clamp-on-link-pin contact, leadscrew/trunnion contact within the clamp and constraints for applied bending moment and pipe flexure during hub misalignment analysis.

Early in the modeling process it was determined that static-general analysis was not robust enough to attain a stable solution. Dynamic-implicit was therefore chosen to attain a robust and reliable converged solution during the clamp-up and leadscrew pretension phase of the simulation, over-coming initial contact stabilization and convergence problems.

3.2 Mesh Density and Structure

To satisfy contractual obligations, two separate Optima models were created. The first Optima model (parent) would consider the detailed aspects of DuoSeal and clamp contact performance through the in-service load case to qualify the design. As such, the mesh discretization on this parent model from which multiple load cases would be run, was optimized in the contact regions.

The mesh density in the DuoSeal where contact is made on the hub seat area(s) was set to 0.03 inches as a result of a thorough mesh sensitivity analysis. It was found that below this 0.03 inch mesh size, the Von Mises (V.M.) and contact stress profiles in the DuoSeal proved to be largely mesh independent, with deviation from the smallest mesh size considered in the analysis, to the 0.03 inch threshold, of <5 %.

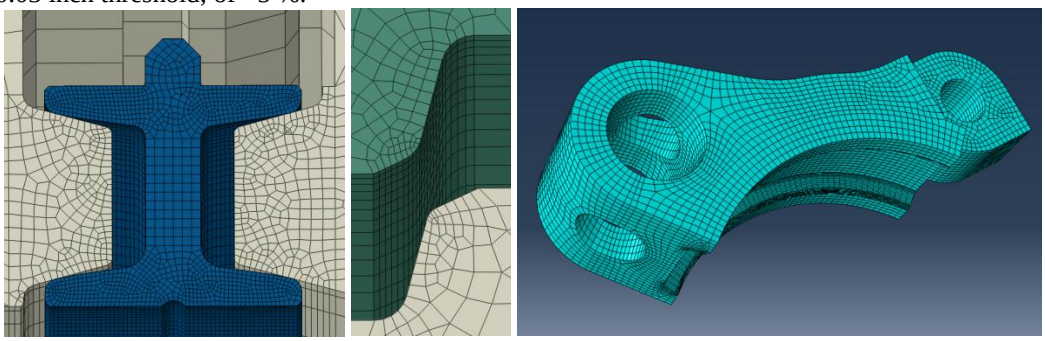

Figure 3: Left to right; mesh density in the DuoSeal and surrounding seat area, mesh density in the contacting clamp and hub region, overview of mesh structure in the lower clamping segment.

The second Optima model considered for the analysis was required to simulate two hub misalignment load cases, where the central axis of the male and female hub(s) was offset by 0.5° and 1°, equally about the central plane through the clamp segments. In this model, a lower mesh density was used in the DuoSeal and other relevant contact areas, with minimal additional

elements concentrated in these contact regions. Figure 3 illustrates the optimized mesh structure for sections of the parent model;

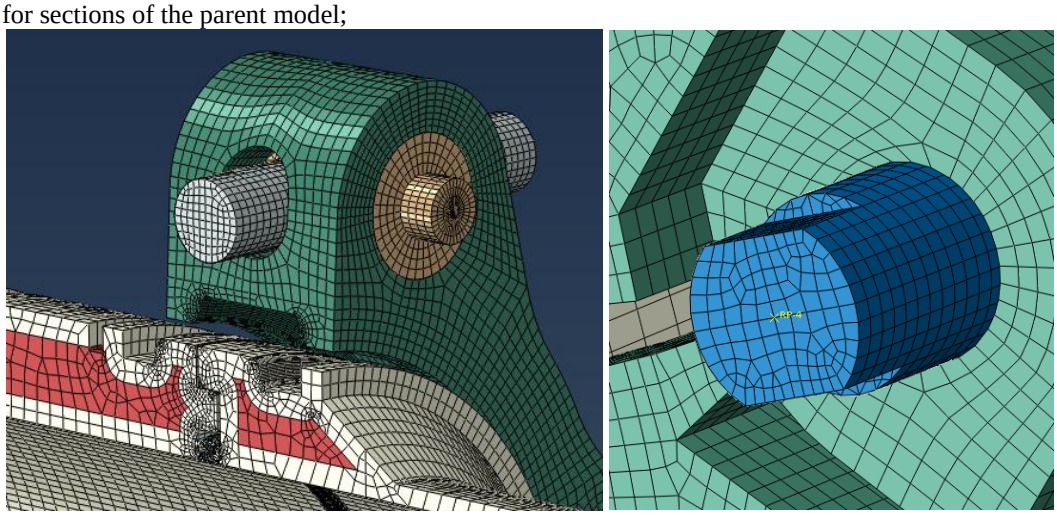

Figure 4: Left to right; General view of parent model global mesh of the No.36 Optima, detailed view of link-pin within upper clamp lug.

In all load cases considered to satisfy customer requirements, the same global mesh density was used containing around 93 % C3D8R hexahedral elements, with the remaining 7 % using C3D4 tetrahedral elements. The misalignment models utilized approximately $380x10^3$ elements with $410x10^3$ nodes. The parent model run with multiple load cases used approximately $445x10^3$ elements with $600x10^3$ nodes, where approximately $1x10^6$ degrees of freedom (DOF) are located in the DuoSeal alone.

3.3 In-service Boundary Conditions

In order to complete the comprehensive structural assessment required for the No.36 Optima, stress profiles of individual components, through the clamp segments ability to pull-in against bending moments and withstand internal pressures must be quantified. The range of individual structural loads are detailed below and documented in Table 2;

I. Internal design pressure of 3,379 Psi (plus internal pressure to yielding).
II. Leadscrew pretension of 787,730 lbf.
III. Axial pipe thrust due to internal pressure 20,013 Psi.
IV. Axial pipe thrust due to mass of the pig launcher of 38,532 Psi.
V. Global bending moment of $4.13x10^6$ lb·ft (plus global bending moment to yielding).
VI. 1° hub misalignment with $7.38x10^6$ lb·ft of pull-in bending moment.
VII. 0.5° hub misalignment with $2.29x10^6$ lb·ft of pull-in bending moment.

Individual components are given a bespoke thermal profile at specified points during all simulations. Throughout all simulations, a friction co-efficient of 0.15 is used on all contacting

surfaces, except for those surfaces where the clamps come into contact with the male and female hubs; this value is increased to 0.25.

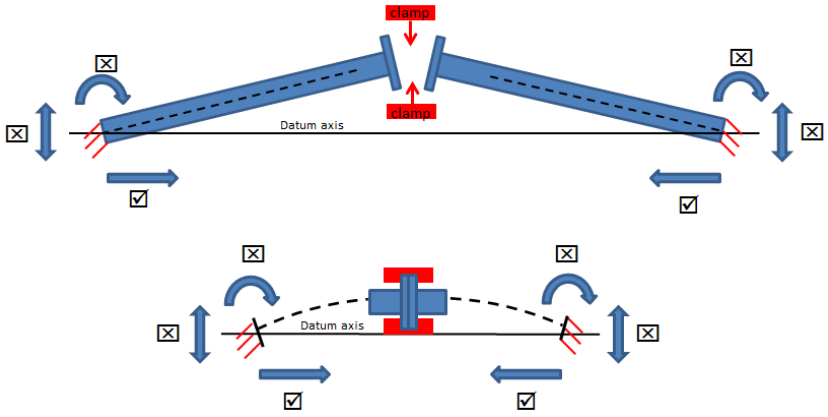

Figure 5: Bending moment schematic for generated hub misalignment.

Table 2: Boundary conditions and temperatures for in-service load case.

Load Case: In-service		Hub Alignment Status: Aligned				
Analysis Step No.		No.1 – Initial Contact	No.2 – Clamp-up & Pull-in	No.3 – Pressurization	No.4 – Hub & DuoSeal Temperature Variation	No.5 – Bending Moment
		Temperature Specification (°C)				
System Component	DuoSeal	-2	-2	-2	+60	+60
	Clamp(s)	-2	-2	-2	-2	-2
	Hub(s)	-2	-2	-2	+60	+60
	Link-pin	-2	-2	-2	-2	-2
	Leadscrew(s)	-2	-2	-2	-2	-2
	Trunnion(s)	-2	-2	-2	-2	-2
		Loading Value (units)				
System Loading	Bending Moment/Axial Thrust due to Pull-in	-	0 lb·ft / 38,532 Psi	0 lb·ft / 38,532 Psi	0 lb·ft / 38,532 Psi	0 lb·ft / 38,532 Psi
	Leadscrew Pretension	-	787,730 lbf	787,730 lbf	787,730 lbf	787,730 lbf
	Pressurization	-	-	3,379 Psi	3,379 Psi	3,379 Psi
	Axial Pipe Thrust (applied as pressure)	-	-	20,013 Psi	20,013 Psi	20,013 Psi
	Global bending Moment	-	-	-	-	4.13×10^6 lb·ft

The modeling of hub misalignment (*see Figure 5*) is considered as an additional capacity check by the customer. Hub misalignment is taken out of the system through the action of the clamping segments wrapping themselves around the male and female hub shoulders. As more contact is made at the primary hub shoulders, hub faces become increasingly parallel, to the point where the clamps are fully positioned and hub misalignment in the system is zero (with hub faces touching).

During this process, the respective male and female hub pipe ends are fixed to the original misalignment angle, but allowed to move freely along the global central axis of the model (*see Figure 5*). As the misalignment is taken out of the hub end, pipe stresses are generated due to induced bending moment. The length of pipes for the 0.5° and 1° alignment simulations are calculated so that hub faces become parallel when maximum pipe bending moment is generated.

3.4 Model Stability Issues and Limitations

Considering the hub misalignment simulations documented in *Section 3.3*, initial problems were encountered with the contact force generated between the secondary shoulders of the clamp segment(s) and hub(s). Point load contact generated early in the clamp-up phase from the leading edges of the upper clamp segment, caused local mesh distortion at the point of contact. Initial modeling for the parallel hub load cases used node-to-surface contact to establish contact stabilization. It was found that as contact force became higher (especially during misalignment load cases), it was better to revert to the surface-to-surface contact algorithm, with a larger time step size used to compensate for the more complex surface contact algorithm.

Local mesh distortion was found to affect the initial movement of the upper clamp(s) around the hub(s), creating local deformations/discontinuities; in the worst instances, the formation of mesh 'spikes' were seen. This dramatically increased solution time, with some trial runs causing a complete lack of solution convergence. Increases in the time step length were employed to reduce these meshing problems.

An initial time step length of 1 was used to monitor solution convergence. Solution convergence was found to be slow, partly down to the meshing 'spikes' mentioned previously, making it harder for primary contact surfaces to move relative to one another. Increasing the time step length from 1 to 10, improved this, and with another increase from 10 to 100, solution convergence became easier, with a reduction in the amount of visible mesh deformation seen on the FEA model. A time step length of 100 was maintained for each of the subsequent load steps, reducing model instabilities, where overheads associated with dynamic implicit, utilizing quasi-static damping effects, are negligible due to the stability achieved through the first load step of the analysis.

Further increases in local radial mesh density of the hub(s) allowed these problems to be reduced to much more manageable levels. A relatively easy fix for the local mesh deformation would have been to increase the mesh density on the affected areas significantly over that originally specified in initial models. The mesh structure in the pipe sections adjoining to the male and female hubs is generally of little interest compared to the DuoSeal and clamps. Consequently, the mesh is coarsened in these areas to improve overall solution speed.

Initial troubleshooting highlighted element distortion in the end of the pipe sections, when specified with the continuum coupling feature for the applied global bending moment. In order to eliminate these convergence problems, full element integration was selected in the mesh of the pipe sections, creating more gauss points, improving the resolution of the element stiffness matrix. The quest for a sufficiently accurate and detailed FEA model, whilst maintaining sensible speed to solution times due to customer timescales, meant that overall high mesh densities were not a viable option. Intelligent use of increased element density in important areas, together with reductions in element numbers in other less critical parts of the FEA model, ensured that global element numbers and DOF did not alter significantly.

4. FEA Validation

In order to justify the simulation techniques and methodology used for analysis of the FEA results generated from the two worst load case requirements; 0.5° and 1° hub misalignment, comparison has been made of the bending stresses induced in the pipes joined to the male and female hubs. A 4.2 % and 2.1 % discrepancy is recorded between hand calculations (for pipe bending under flexure and applied moment) and Abaqus/CAE for the 0.5° and 1° misalignment load case respectively. Similar comparisons have been made between the in-service load case and theory, with discrepancies between theory and Abaqus/CAE being almost negligible.

5. Simulation Results

5.1 Von Mises Stress Results of In-service Analysis

Figure 6 shows the overall FEA stress profile of the No.36 Optima, generated at the end of the general operation (in-service) load case documented in Table 2;

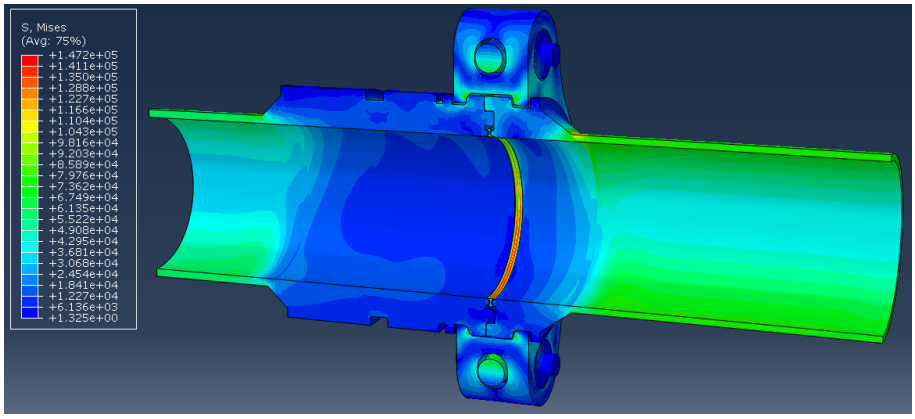

Figure 6: Global V.M. Stress plot (Psi) for the No.36 Optima.

Figure 6 shows that most stresses in the Optima (DuoSeal excluded) are relatively low, with high stress regions present around the primary contact shoulders between the male and female hubs, and the corresponding contact regions with respective clamps. The higher stress found along the lengths of the pipe work is the result of applied bending moment together with internal pressure.

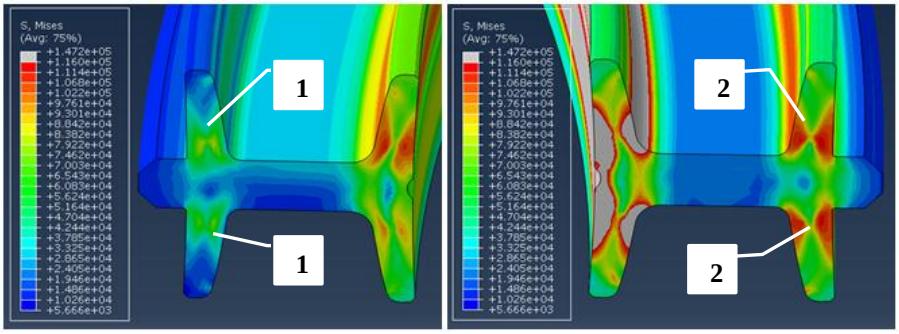

Figure 7: Left to right; V.M. Stress plot (Psi) of the upper DuoSeal region in the No. 36 Optima DuoSeal showing local regions of plastic deformation (grey), V.M. Stress plot (Psi) of the lower DuoSeal region in the No.36 Optima DuoSeal showing local regions of plastic deformation (grey).

Figure 7 illustrates the V.M stresses in the DuoSeal, generated at the end of the application of global bending moment on the FEA model. The inner portions of the DuoSeal are highly stressed, but significantly lower stresses (compared to the respective inner regions) are seen on the outer heel sections of the DuoSeal (*see inset Figure 7*; labels (**1**) and (**2**)).

As is expected from the application of bending moment, the left hand image of Figure 7 shows a variation of stress that reduces both outward through the radius, and anticlockwise through the bending angle. This generates increased compressive stresses in the lower portion of the DuoSeal (*see right hand side image of Figure 7*), both on the upper and lower heel sections of this portion of the DuoSeal. In this particular scenario, the inner heel regions deform plastically. This enables the DuoSeal to generate a larger sealing area when excessively stressed, promoting better sealing performance when subjected to the in-service operational loadings.

5.2 DuoSeal Contact Pressure Results of In-service Analysis

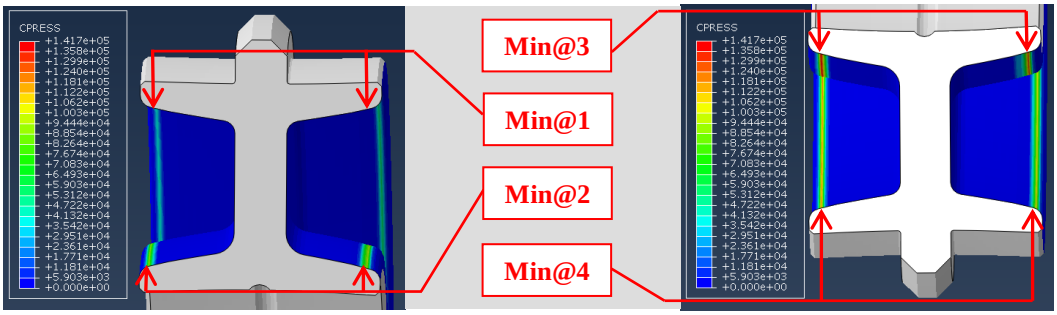

Figure 8: Left to right; Illustration of seat contact pressure (Psi) on the top portion of the DuoSeal at the end of analysis step No. 5 and on the bottom portion of the DuoSeal at the end of analysis step No.5 (*see Table 2*).

In Figure 8, Min@1, Min@2, Min@3 and Min@4 are representative of the maximum contact stresses recorded at the four individual sealing points on the upper and lower sections of the DuoSeal, as in the FEA model shown in Figure 2. Of these contact stresses, the minimum of the maximum values of the four data sets are plotted in the contact pressure graph (*see Figure 9*).

Very good sealing performance is illustrated in Figure 8 whereby the inner portions of both the upper and lower regions of the DuoSeal have a much wider contact area than the outer portions, with the right hand side image of Figure 8 showing distinctive high banding contact stresses, consistent with the V.M. stress patterns shown in Figure 7. Figure 9 illustrates the variation in DuoSeal contact stress through the complete range of operation;

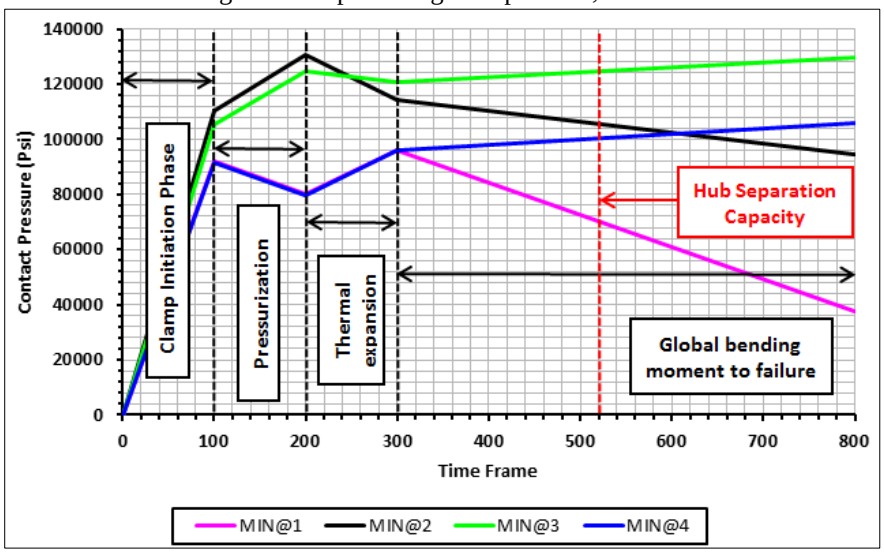

Figure 9: Graph of DuoSeal contact pressure during the stages of the simulation for the general operational in-service load case of Table 2.

Figure 9 shows the contact pressure profile on the DuoSeal through to the end of the global bending moment capacity test, where the bending moment capacity was run to 7.08×10^6 lb·ft. Once the clamp-up phase is complete, subsequent system loadings generate contact stresses on the important inner heel areas of the DuoSeal that never drop below approximately 80,000 Psi, higher than customer requirements for contact stress. The global bending moment to cause loss of hub face contact pressure, and subsequent hub face separation is approximately 4.96×10^6 lb·ft.

5.3 Structural Capacity Analysis

In order to generate an official structural rating for the No.36 Optima under the specific loading conditions of Table 2, it must exceed both the pressure and bending moment design criteria imposed by the customer. The bending moment and pressure capacity tests (each undertaken in isolation) are subjected to 1.67x107 lb·ft and 10,000 Psi respectively. In these tests, the clamp-up phase of the Optima is simulated, then either the bending moment or pressure capacity is applied to the Optima until hub separation or yielding occurs.

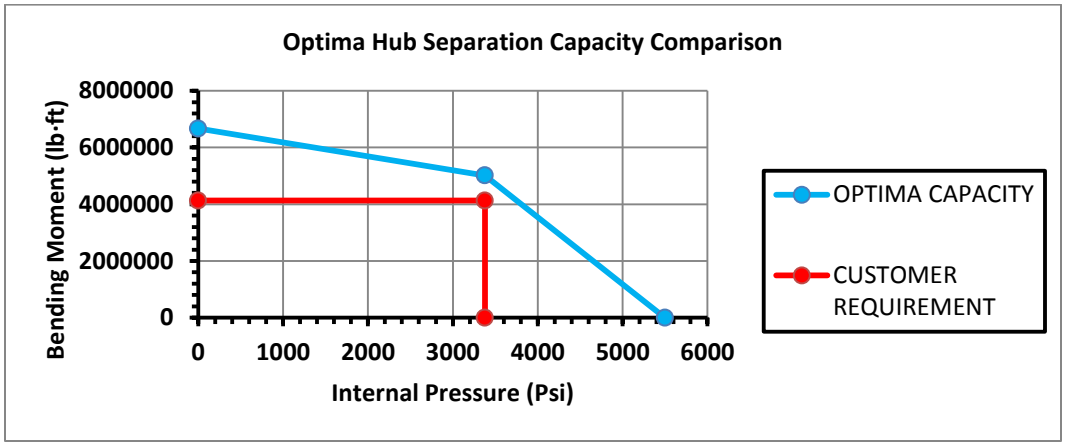

Figure 10: Graph of hub separation capacity for the No.36 Optima subsea connector.

Figure 10 shows the No.36 Optima can withstand 61.4 % more bending moment and 62.7 % more internal pressure than required by the customer. Adequate sealing contact pressure is still maintained even after the separation of hub faces (*see Figure 9*).

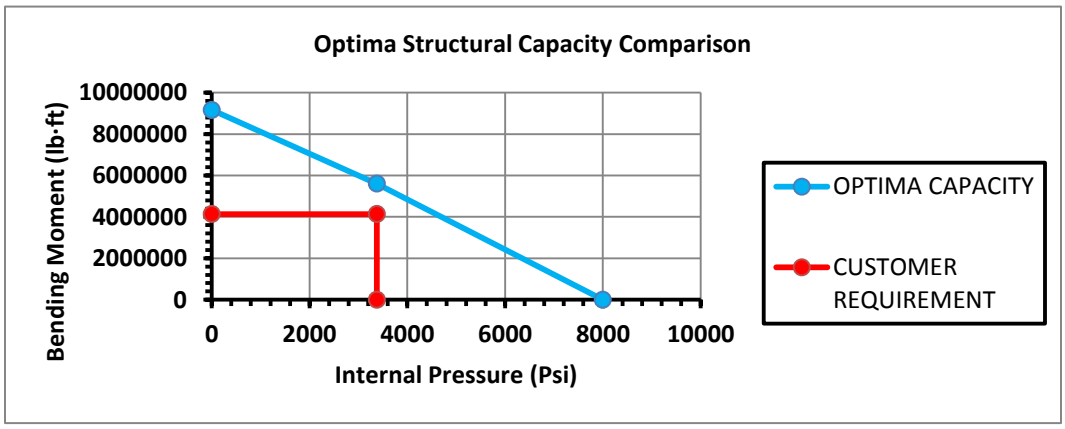

Figure 11: Graph of structural capacity for the No.36 Optima subsea connector.

Figure 11 shows the structural capacity of the No.36 Optima, based on local plastic strain within the components. The graph shows that the Optima can withstand 121.9 % more bending moment and 195.7 % more internal pressure than required before the onset of plastic strain.

During the analysis required to determine the data for Figure 11, it was noted that plastic strain is always present within the DuoSeal and is therefore eliminated from the predictions of Figure 11. It is also noted that the trailing and leading edges of the clamp segments cause very small localized

areas of plastic strain, but these strains are present only at the surface of the components. Therefore, plastic strain generated as a result of the trailing and leading edges of the clamp segments is also eliminated from these predictions.

5.4 Hub Misalignment Analysis

Clamp qualification through reduction in hub misalignment is in fulfillment of a scenario where the pipeline and No.36 Optima are not able to be brought parallel for initial clamp-up and mechanical energisation of the DuoSeal. For the hub misalignment load case, there is no internal pressure or external global bending moment requirements for the simulation. Figure 12 illustrates the stress profile through the 1° hub misalignment load case, and shows an expected difference in stress levels in the two pipes as a result of the difference in their respective lengths and pipe wall thicknesses;

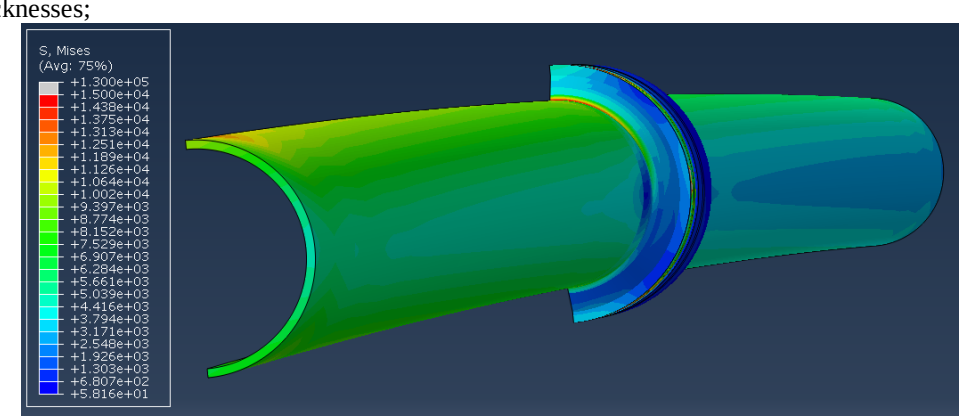

Figure 12: V.M. Stress plot (Psi) in the pipework and male and female hub components after reduction from 1° to 0° of hub misalignment.

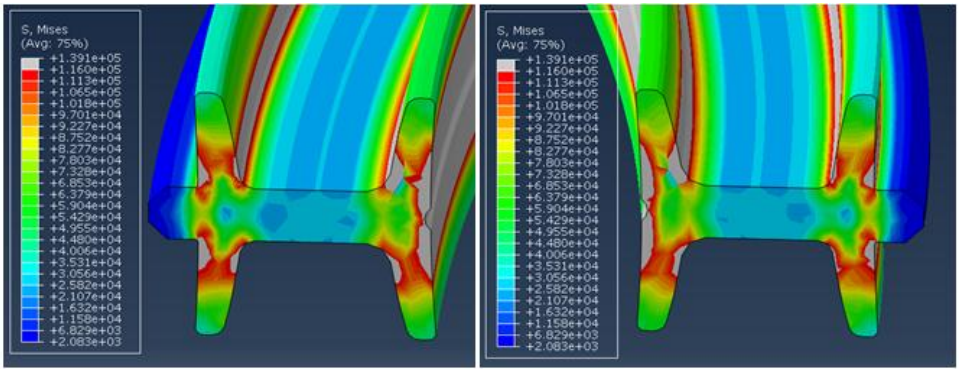

Figure 13: Left to right; V.M. Stress plot (Psi) of the upper DuoSeal region in the No.36 Optima DuoSeal showing local regions of plastic deformation (grey), V.M. Stress plot (Psi) of the lower DuoSeal region in the No.36 Optima DuoSeal showing local regions of plastic deformation (grey).

Figure 13 shows that the V.M. stresses generated from clamp-up show large areas of plastic deformation in both the upper and lower portions of the DuoSeal. This acts as a sanity check for the hub misalignment load cases, indicating that the male and female hubs have been brought together properly by the action of the clamp segments, showing that the clamp segments are generating equal load through the hubs, reacting onto the DuoSeal.

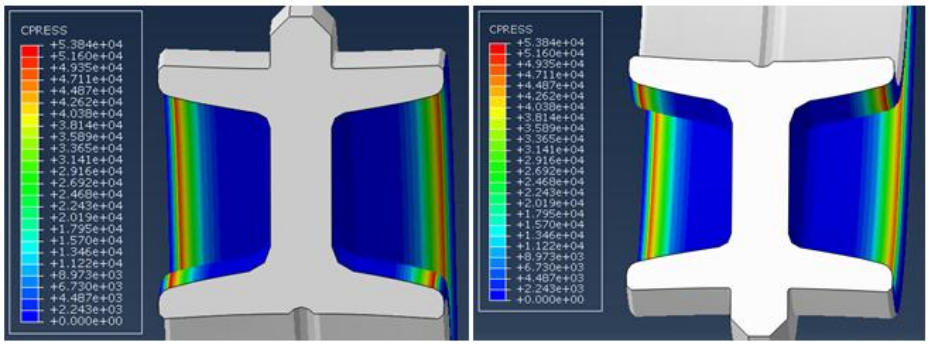

Figure 14: Left to right; Illustration of seat contact pressure (Psi) on the top portion of the DuoSeal at the end of the FEA simulation, Illustration of seat contact pressure (Psi) on the bottom portion of the DuoSeal at the end of the simulation.

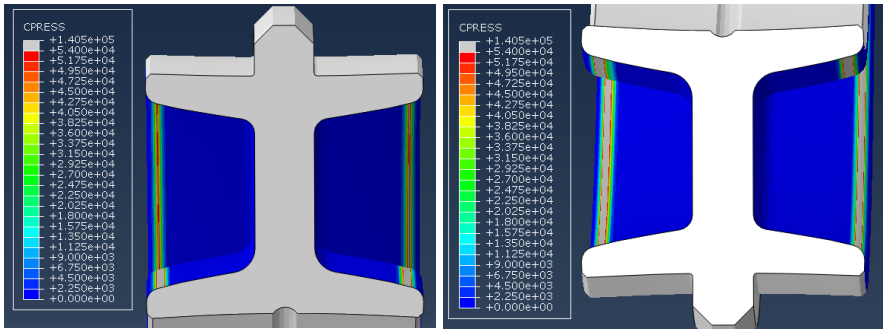

Figure 15: Left to right; Illustration of seat contact pressure (Psi) on the top portion of the DuoSeal during in-service clamp-up, Illustration of seat contact pressure (Psi) on the bottom portion of the DuoSeal during in-service clamp-up.

Discrepancies between Figure 14 and Figure 15 can be attributed to the mesh density used within the DuoSeal. Both load cases illustrate that the stress banding is consistent around the whole diameter of both the upper and lower, inner and outer sealing regions of the DuoSeal. Therefore, the comparative analysis shows that the modeling assumptions that have been used are correct, even if the magnitude of values generated through the FEA simulations are dissimilar.

6. Conclusion and Future Work

This paper has documented the detailed set-up required to produce the simulation load cases required for the No.36 Optima. FEA simulation results indicate that the collective design of all

components meets the bending moment and internal pressure capacity criteria set out by the customer. The simulation results have demonstrated the ability of the No.36 Optima to successfully pull-in against the static weight of the pig launcher, together with a range of hub misalignments up to 1°, representing discrepancies in pipeline global positioning. It has been shown that the integrity of the DuoSeal is maintained throughout the required load cases, producing contact stresses that exceed requirements. Fatigue analysis for component life cycles has not been required due to the in-service steady state loadings on the No.36 Optima.

The analysis has allowed FO&GT to make predictions where important areas of large elastic/plastic strain may occur during the factory qualification process. Validation of the FEA results will help to further improve the analysis process for future applications. Strain gauging equipment can be positioned during the factory qualification process to accurately monitor plastic deformation. Rigorous checking of factory performance figures against the analysis predictions in this report will ensure that areas/results/data that agree/disagree with simulation reference data are identified, with subsequent steps taken to rectify the correlations obtained.

7. References

1. Bates A., Mukherjee S., Hwang S., Lee S.C., Kwon O., Choi G.H., Park S. “Simulation and Experimental Analysis of the Clamping Pressure Distribution in a PEM Fuel Cell Stack”, International Journal of Hydrogen Energy 38, pp. 6481-6493, 2013.
2. Dassault Systems Abaqus 6.12, Abaqus/CAE User's Guide, Providence: [s.n.], 2013.
3. Hilber H.M., Hughes T.J.R., “Collocation, Dissipation and 'Overshoot' for Time Integration Schemes in Structural Dynamics”, Earthquake Eng. Struct. Dyn. 6, pp. 99-117, 1978.
4. Kyun C. Woo K., Shim J., “Analysis of Contact Force and Thermal Behaviour of Lip Seals”, Tribology International 30, pp. 113-119, 1997.
5. Lee C.Y., Lin C.S., Jian R.Q., Wen C.Y., ”Simulation and Experimentation on the Contact Width and Pressure Distribution of Lip Seals”, Tribology International 39, pp. 915-920, 2006.
6. Rebelo N., Nagtegaal J.C., Taylor L.M., “Comparison of Implicit and Explicit Finite Element Methods in the Simulation of Metal Forming Processes: Numerical Methods in Industrial Forming Processes”, Chenot, Wood, Zienkiewicz, 1992.
7. Sanal Z., “Nonlinear Analysis of Pressure Vessels: Some Examples” International Journal of Pressure Vessels and Piping 77, pp. 705-709, 2000.
8. Sun J.S., Lee K.H., Lee H.P., “Comparison of Implicit and explicit Finite Element Methods for Dynamic Problems”, Journal of Materials Processing Technology. 105, pp. 110-118, 2000.

8. Acknowledgements

I would like to thank all individuals and companies involved in the creation of this paper. I would especially like to thank my co-author Mr. Laurence Marks for his support and guidance with the simulation aspects of this project. I would also like to thank Mr. John Stobbart (Technical Director) and Mr. Nick Long (Subsea Technical Authority) for their expertise in the design of the DuoSeal and No.36 Optima.